DFT studies of two-electron oxidation, photochemistry, and radical transfer between metal centres in the formation of platinum(IV) and palladium(IV) selenolates from diphenyldiselenide and metal(II) reactants

Allan J. Canty,*[a] Alireza Ariafard [a] and Richard J. Puddephatt [b]

DFT computation indicates that the oxidant diphenyldiselenide reacts with palladium(II) and platinum(II) complexes $MMe_2(bipy)$ (bipy = 2,2'-bipyridine) to form a pre-equilibrium involving weak adducts, from which $[MMe_2(bipy)]_2{\cdot}Ph_2Se_2$ undergoes rate-limiting dissociation of phenylselenide preceded by the oxidative addition step to obtain $[Me_2(bipy)M\text{-}MMe_2(bipy)(SePh)]^+$. Coordination of $PhSe^-$ gives the neutral M^{III}-M^{III} bonded dimers $[MMe_2(bipy)(SePh)_2]_2$. The dimers fragment in the presence of light to give radicals $[M^{III}Me_2(bipy)(SePh)]^\bullet$ via excitation to states with M-M antibonding character. After reorientation in the solvent cage, the radicals interact to form triplet adducts $[M^{III}Me_2(bipy)(SePh){\cdot}(bipy)M^{III}Me_2(SePh)]^{\bullet\bullet}$ with π-stacked 'SePh·bipy', followed by transformation via a Minimum Energy Crossing Point allowing $[SePh]^\bullet$ transfer to give $M^{II}Me_2(bipy)$ and $M^{IV}Me_2(bipy)(SePh)_2$. The regenerated M^{II} reagent reacts with Ph_2Se_2 through the above sequence, allowing completion of reaction to give M^{IV} product only. The reaction of $PtMe_2(bipy)$ with diphenyldisulfide has been studied in an analogous manner to assist with interpretation of DFT results for reactions of diphenyldiselenide.

Introduction

Studies of oxidation of diorganoplatinum(II)[1-3] and palladium(II) complexes[2] by diselenides RSeSeR have elicited a well-developed structural chemistry for 2'2'-bipyridine (bipy) and 1,10-phenanthroline (phen) as auxiliary ligands in complexes $M^{IV}R_2(N\sim N)(SePh)_2$ (Scheme 1a).[1,2a,c] The reactions are considered to be model reactions for some roles of these transition metals in organic synthesis.[4] There is scarce evidence for the mechanism of oxidation by diselenides in these reports, although reactions are proposed to occur at least partly by free radical processes.[1;2a,c] However, for the related dichalcogenide diphenyldisulfide, experimentation has demonstrated that binuclear platinum(III) species $[PtMe_2(N\sim N)(SPh)]_2$ are formed as intermediates in a 'one-pot' stepwise process to give Pt^{IV} products (Scheme 1b).[5] The step forming the dimers does not appear to proceed via radicals (failure to observe CIDNP effects in NMR spectra, no induction period or retardation of reaction by free radical scavengers), but a radical mechanism is implicated for conversion of dimers to $Pt^{IV}Me_2(N\sim N)(SPh)_2$ (reactions faster in the light than in the dark).[5] Disproportionation of isolated $[Pt^{III}Me_2(phen)(SPh)]_2$ to the Pt^{II} reagent and Pt^{IV} product has been demonstrated (Scheme 1c), and this process is assumed to play a role in the 'one-pot' synthesis where there is sufficient Ph_2S_2 to react with the Pt^{II} reagent thus formed (Scheme 1b).

Scheme 1 on page 2

A computational study reported by one of us[5] elucidated the mechanism to form Pt^{III} thiolate dimers (Scheme 1d),[5] abbreviated here to show only the key species. The formation of several weak adducts is followed by inner-sphere oxidative transfer of $[PhS]^+$ to a Pt^{II} centre of the adduct $Me_2(bipy)Pt{\cdot}PtMe_2(bipy){\cdot}S_2Ph_2$, and subsequent coordination of $[PhS]^-$ at the other Pt centre to give the neutral symmetrical dimer.[5] The mechanism for the disproportionation reaction has not been established.

The experimental and computational results for the reaction of $Pt^{II}Me_2(bpy)$ with Ph_2S_2 raise several fascinating questions that may be addressed computationally for both palladium and platinum: (a) do $M^{II}Me_2(bipy)$ react with Ph_2Se_2 in the same stepwise manner as found for $Pt^{II}Me_2(bipy)$ with Ph_2S_2, (b) what is the mechanism of the proposed photochemically initiated process for the disproportionation of $[Pt^{III}Me_2(bipy)(SPh)]_2$, and does this occur for the selenium systems, and (c) are there differences in mechanism for palladium and platinum?

We find that a singlet pathway for oxidation by Ph_2S_2 to form the Pt^{III} dimer abbreviated in Scheme 1d applies for Ph_2Se_2. The neutral M^{III} dimers undergo photochemical excitation leading to homolytic fragmentation from an excited state with M-M antibonding character to form two doublets $[M^{III}Me_2(bipy)(SePh)]^\bullet$. The doublets react together in a process involving $[PhSe]^\bullet$ transfer to give $M^{II}Me_2(bipy)$ and $M^{IV}Me_2(bipy)(SePh)_2$.

---

[a] *School of Natural Sciences – Chemistry, University of Tasmania, Private Bag 75, Hobart, Tasmania 7001, Australia. E-mail:allan.canty@utas.edu.au*

[a] *Department of Chemistry, University of Western Ontario, London, Canada N6A 5B*

† Electronic Supplementary Information (ESI) available: CCDC XX-XX Energy profiles, Gaussview diagrams, orbitals, TD-DFT data, energy parameters and Cartesian coordinates are provided. See DOI: xxxxxxxxxx

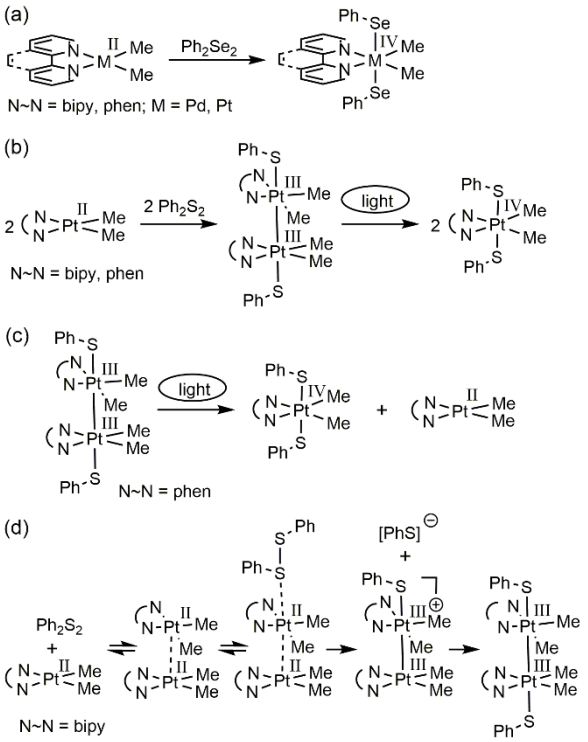

Scheme 1 (a) Synthesis of $M^{IV}Me_2(N\sim N)(SePh)_2$ complexes for which X-ray crystal structures are reported for Pt [1,2a] and a pallada(IV)cyclopentane analogue,[2a] (b) stepwise formation of Pt^{IV} thiolate complexes via isolable Pt^{III} dimers in 'one-pot' reactions,[5] (c) disproportionation of an isolated Pt^{III} complex in acetone, and (d) schematic of the computational study for formation of $[Pt^{III}Me_2(bipy)(SPh)]_2$. Computation indicates the presence of additional adducts $[Pt^{II}Me_2(bipy)\cdot S_2Ph_2]$ and $[Pt^{II}Me_2(bipy)\cdot S_2Ph_2\cdot Pt^{II}Me_2(bipy)]$.[5]

Experimental section

Gaussian 16[6] was used at the M06 level of Density Functional Theory (DFT) for geometry optimisation in view of the presence of dispersion associated with the formation of adducts involving aromatic rings in close proximity and metal-metal interactions.[7] The Stuttgart/Dresden ECP (SDD) was used to describe Pd, Pt, and Se,[8] and the 6-31G(d) basis set was used for other atoms to form basis set BS1. Computation was carried out for the experimentally employed solvent acetone utilising the IEFPCM (SCRF) model. To further refine energies obtained from the M06/BS1 calculations, we carried out single point energy calculations for all structures at the M06 level incorporating Grimme's D3 computation to account more completely for dispersion[9]. These calculations employed a larger basis set (BS2) utilising the quadrupole-ξ valence polarized def2-QZVP[10] basis set on Pd, Pt and Se along with the corresponding ECP and the 6-311+G(2d,p) basis set on other atoms. All thermodynamic data were calculated at the standard state (298.15 K and 1 atm). To estimate the corresponding Gibbs free energies in acetone, entropy corrections were calculated at the M06/BS1 level and added to the single point potential energies. An additional correction for compression of 1 mol of an ideal gas from 1 atm to the 1 M solution phase standard state (1.89 kcal mol^{-1})[11] was applied. Transition structures contained one imaginary frequency, exhibiting atom displacements consistent with the anticipated reaction pathway. The nature of transition structures was confirmed from potential energy surface scans. TD-DFT computation was performed with CAM-B3LYP[12] and BS1. Further details are given in the ESI.

Results and Discussion

Reactions of $M^{II}Me_2(bipy)$ with Ph_2Se_2

Computation commenced with an exploration of potential pathways for the reaction of $PtMe_2(bipy)$ using the model developed for reaction with Ph_2S_2 (Scheme 1c). The preferred singlet sequence found for Ph_2Se_2 is shown in black in Fig. 1a. Exergonic formation of the dimer $[PtMe_2(bipy)]_2$ (**2a**) (ΔG -5.6 kcal mol^{-1}) reflects the occurrence of this dimer in the crystalline state.[13] A pre-equilibrium is represented by **2a** ⇌ **3a** ⇌ **4a** ⇌ **5a**.

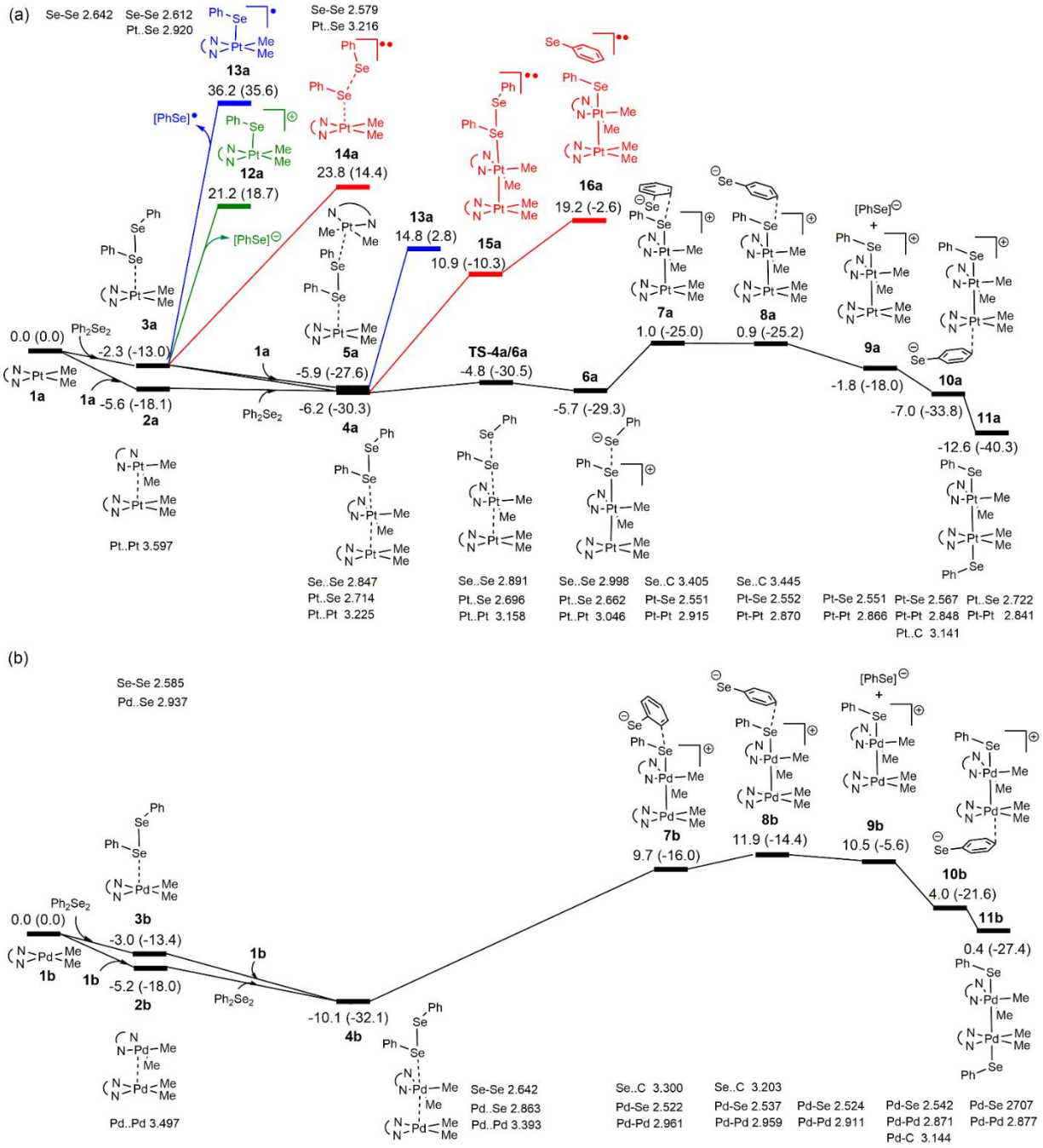

Fig. 1 Energy profile for the reaction of Ph_2Se_2 with (a) $PtMe_2$(bipy) and (b) $PdMe_2$(bipy), illustrating the lower energy singlet pathways in black, and initial species in higher energy singlet (green), doublet (blue) and triplet (red) pathways for platinum. For (b), only lower energy singlet species are illustrated. Selected interatomic distances are shown in Å, and energies ΔG (ΔH) are in kcal mol^{-1}.

The barrier for oxidation is remarkably low (*ca*. 1.4 kcal mol^{-1}), assisted by the second Me_2Pt(bipy) unit in **4a** (neighbouring group effect) that also allows formation of a binuclear Pt^{III}-Pt^{III} product **6a**, in marked contrast to direct oxidation at a mononuclear site in **3a** to give **12a** (ΔG 23.5 kcal mol^{-1}).

Structure **6a** exhibits a Pt-Se distance of 2.662 Å, only *ca*. 0.14 Å longer than that for the dimeric Pt^{III} product **11a** (2.722 Å), and the Pt-Pt distance is reduced by *ca*. 0.18 Å. Bonding in the Pt^{III} structure **6a** can be represented as resonance forms (Fig. 2a), and by a molecular orbital scheme (Fig. 2b) in which the HOMO of $[PhSe]^-$ interacts with the LUMO of the cation $[(bipy)Me_2Pt\text{-}PtMe_2(bipy)(SePh)]^+$ (**9a**).

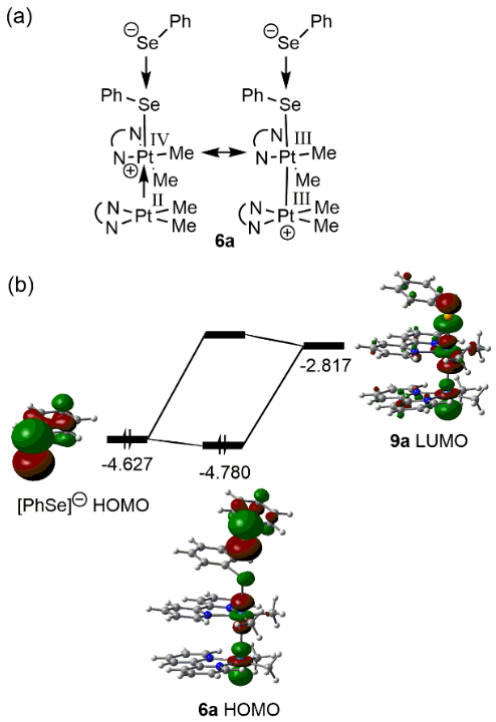

Fig. 2 Resonance (a) and molecular orbital representations (b) of bonding in the first formed Pt^{III} intermediate **6a**. Energies in eV.

A transition state for completion of the departure of $[PhSe]^-$ from **6a** could not be located. Potential energy scans located ion pair adducts **7a** and **8a**, and indicate a barrier of ΔE <1 kcal mol^{-1} (basis set BS1) for **7a** returning to **6a**. Ion pair **10a** is also a feasible adduct on the pathway to form **11a**. Although the precise nature and sequence of intermediates between **6a** and product **11a** is elusive, the barrier for formation of **7a** from the lowest energy structure in the pre-equilibrium (**4a**) is estimated to be around *ca*. *G* 7.2 kcal mol^{-1}.

We also explored additional mechanisms, including initial species for radical pathways although experimental data indicate that such mechanisms are unlikely. Results are shown in colour in Figure 1a. They all computed as very high energy compared with the singlet sequence in black: (a) singlet oxidative transfer of $[PhSe]^+$ in **3a** to form **12a**, mentioned earlier, (b) homolytic dissociation of **3a** to form doublet **13a**, (c) formation of **14a** from **3a** to commence a pathway involving triplets, (d) formation of doublet **13a** from **5a**, and (e) formation of **15a** from **4a** to commence another pathway involving triplets. In addition, for the heterolytic dissociation (**3a** → **12a** + $[PhSe]^-$) and homolytic dissociations (**3a** → **13a** + $[PhSe]^\bullet$, **5a** → 2 **13a**), very high barriers ΔG can be estimated (31.7, 48.6 and 30.4 kcal mol^{-1}, respectively) from the change in ΔH for these processes following the protocol developed by Hartwig and Hall.[14]

An analogous pathway for the reaction of $PdMe_2(bipy)$ was found (Fig. 1b), and in this case species higher than the singlet pathway are omitted (analogues of **12a** – **16a**, details in ESI). The singlet pathway illustrates presence of pre-equilibria followed by an oxidative process from adduct **4b**. A transition state for dissociation of $[PhSe]^-$ from adduct **4b** could not be located, but potential energy scans from **7b** back to **4b** indicate a low barrier for this process (ΔE *ca*. 2.8 kcal/mol at BS1).

The energy profile for reaction of $PtMe_2(bipy)$ with Ph_2Se_2 is similar to that for the analogous reaction with Ph_2S_2 (details in ESI). Computation supports the absence of radical pathways for Ph_2S_2, in a similar manner documented above for the Pt/Se system, consistent with experimental evidence for the absence of a radical mechanism for the reaction of Ph_2S_2 to form $[Pt^{III}Me_2(bipy)(SPh)]_2$ (**11c**).[5] A comparison of activation barriers and overall ΔG for the reactions studied (eq 1) is given in Scheme 2. In all cases the resting state for reactants is $[Me_2M^{II}(bipy)]_2{\cdot}Ph_2E_2$, e.g. **4a** and **4b** in Fig. 1.

$$\underset{\textbf{1a-c}}{2\ M^{II}Me_2(bipy)} + Ph_2E_2 \rightarrow \underset{\textbf{11a-c}}{[M^{III}Me_2(bipy)(EPh)]_2} \qquad (1)$$

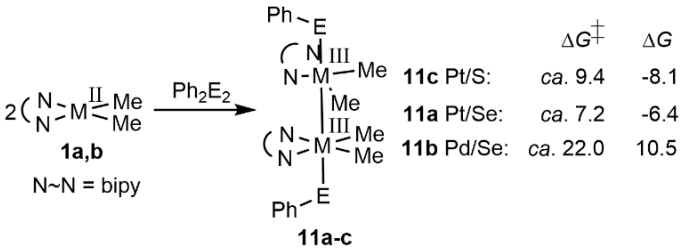

Scheme 2 Comparison of activation parameters and overall ΔG computed for reaction of Ph_2E_2 with $M^{II}Me_2(bipy)$ to form M^{III} dimeric species **11a-c**. Energies in kcal mol^{-1}.

Key Gibbs parameters for the reactions of $PtMe_2(bipy)$ are similar (Scheme 2). However, the reaction of $PdMe_2(bipy)$ has a much higher barrier and the reaction is endergonic, reflecting lower reactivity of the palladium complex toward oxidation. A subsequent photochemical reaction allows disproportionation to proceed exergonically from **11b** for palladium, as discussed below. The unfavourable process for formation of $[Pd^{III}Me_2(bipy)(SePh)]_2$ (**11b**) is consistent with the inability to detect this intermediate in low temperature NMR studies during the synthesis and isolation of $Pd^{IV}Me_2(bipy)(SePh)_2$.[2a]

Disproportionation Reactions of $[M^{III}Me_2(bipy)(EPh)]_2$ (11a-c) promoted by light

Computation for the systems examined here indicate that the disproportionation of the neutral dimers **11-a-c** is exergonic (eq 2).

$$\underset{\textbf{11a-c}}{[M^{III}Me_2(bipy)(EPh)]_2} \rightarrow \underset{\textbf{17a-c}}{M^{IV}Me_2(bipy)(EPh)_2} + \underset{\textbf{1a-c}}{M^{II}Me_2(bipy)} \quad (2)$$

ΔG: -3.9 (**11a**), -8.1 (**11b**), -2.6 (**11c**)

Initially, we examined the $PtMe_2(bipy)/Ph_2S_2$ system for which a photochemical reaction involving radicals has been proposed earlier (Scheme 1b,c).[5] The reaction is assumed to proceed via cleavage of the Pt-Pt bond to give two doublets, $[Pt^{III}Me_2(bipy)(SPh)]^{\bullet}$ (**13c**). Thermochemical formation of **13c** from dimer **11c** is unfavourable, with a barrier estimated as ΔG 45.8 kcal/mol using the Hartwig-Hall protocol[14] described above ($\Delta G^{\ddagger} \sim \Delta H$). Similar high barriers are estimated for analogous fragmentation in the Pt/Se system (ΔG 43.1 kcal/mol, estimated from ΔH for **11a** → **13a**, Fig.1a), and the Pd/Se system (ΔG 31.9 kcal/mol, see ESI for details of Pt/S and Pd/Se systems).

To explore photochemical processes, we undertook TD-DFT computation to identify excited states for $[Pt^{III}Me_2(bipy)(SPh)]_2$ (**11c**), and examined these results together with the nature of unoccupied orbitals in energy immediately above the HOMO (Fig. 3). The HOMO illustrates Pt-Pt bonding. The LUMO+2 has antibonding Pt-Pt character, and is thus a suitable orbital to facilitate bond cleavage. The computation revealed a HOMO→LUMO+2 charge-transfer transition with a maximum absorption at λ 393 nm and a very high oscillator strength (f = 1.7). Lower energy transitions examined (first and second) have low oscillator strengths (f = 0.02, 0.03) involving orbitals unsuitable for facilitating Pt-Pt bond cleavage (combinations of LUMO and LUMO+1). Thus, it was not surprising that optimisation of the excited state related to LUMO+2 (third excitation) led directly to fragmentation, giving 'PtMe2(bipy)' planes facing each other with Pt···Pt *ca*. 4.3 Å, *ca*. 1 Å greater than van der Waals contact (Pt radius = 1.73 Å).[15]

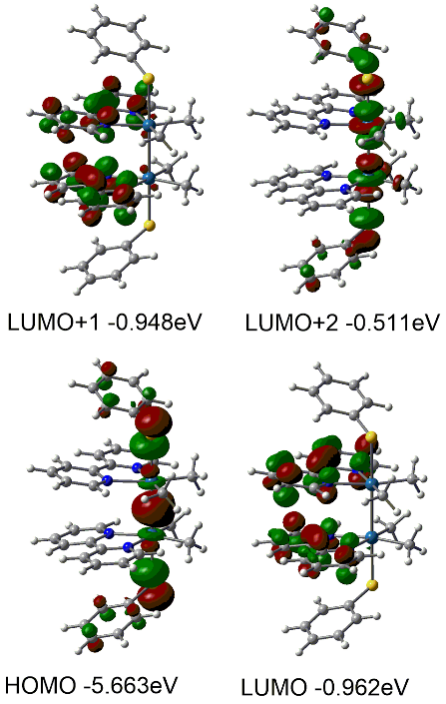

Fig. 3 Gaussview diagrams together with energies for the HOMO and first three LUMO's of $[Pt^{III}Me_2(bipy)(SPh)]_2$ (**11c**).

Similar excited states were obtained for $[Pt^{III}Me_2(bipy)(SePh)]_2$ (**11a**), and orbitals are also similar except that the LUMO and LUMO+1 exhibit orbital distributions located almost exclusively at one bipy group or the other bipy group. The HOMO→LUMO+2 transition (λ = 418 nm, f = 1.75) corresponds to excitation to the Pt-Pt antibonding orbital. However, optimisation of this transition as an excited state resulted in crossing to the lowest excited state, a phenomenon often encountered in this computation process.[16]

For $[PdMe_2(bipy)(SePh)]_2$ (**11b**), excited states and orbitals are similar to those in Fig. 3 except that the Pd-Pd antibonding orbital is the LUMO. The transition to the LUMO corresponds to the first excitation with f 1.52. Optimisation of this excited state results in Pd-Pd cleavage in a similar manner to that described above for $[Pt^{III}Me_2(bipy)(SPh)]_2$. Notably, the weaker Pd-Pd bond also causes the excitation of the Pd^{III} dimer **11b** to be achieved at a lower energy (λ 547 nm) than for the Pt^{III} analogue **11a** (λ 418 nm) and $[Pt^{III}Me_2(bipy)(SPh)]_2$ **11c** (λ 393 nm). The photochemical generation of radicals is represented in eq 3 as a reversible process, owing to the suitable orientation of '$MMe_2(bipy)$' planes for the adjacent separated doublets allowing recombination.

$$\underset{\textbf{11a-c}}{[M^{III}Me_2(bipy)(EPh)]_2} \overset{\text{light}}{\rightleftharpoons} 2\ \underset{\textbf{13a-c}}{[M^{III}Me_2(bipy)(EPh)]^{\bullet}} \qquad (3)$$

We turn now to consideration of the reaction of $[M^{III}Me_2(bipy)(EPh)]^{\bullet}$ doublets (**13a-c**) to facilitate the disproportionation reaction. As the reactions involve transfer of $[EPh]^{\bullet}$ from one metal centre to another, we explored the potential formation of triplet adducts by two doublets, and potential subsequent spin pairing in concert with $[EPh]^{\bullet}$ transfer to give singlet products. The process explored is illustrated for the Pt/Se system in Scheme 3. Formation of a triplet adduct (**18a**) is exergonic, and a singlet product adduct was also found (**19a**), together with a Minimum Energy Crossing Point (**MECPa**) connecting the two adducts. The weak interactions between the two doublets in **18a** and two singlet fragments in **19a** correspond to π-stacking, with the shortest distances illustrated in Scheme 3. **MECPa** has an intermediate structure, illustrating for the $[SePh]^{\bullet}$ group being transferred a decrease in Pt···Se from non-bonding in **18a** (4.046 Å) to van der Waals contact in **MECPa** (3.558 Å) to Pt^{IV}-Se bonding in **19a** (2.587 Å). The activation energy for this process, from **18a**, computes as approximately 1.4 kcal/mol, and thus the transformation from two doublets (**13a**) to the singlet adduct **19a** is regarded as essentially barrierless.

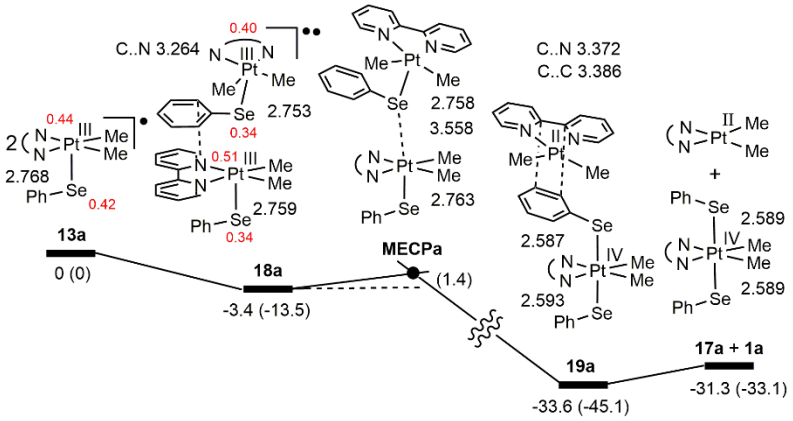

Scheme 3 Reaction of $[Pt^{III}Me_2(bipy)(SePh)]^\bullet$ (**13a**) doublets forming a triplet adduct (**18a**) that undergo spin pairing via a Minimum Energy Crossing Point (**MECPa**) to form adduct (**19a**) comprising $Pt^{IV}Me_2(bipy)(SePh)_2$ (**17a**) and $Pt^{II}Me_2(bipy)$ (**1a**). Spin densities > 0.1 e Å^{-3} are shown in red, together with selected interatomic distances (Å). Energies ΔG (ΔH) are in kcal mol^{-1}, except for **MECPa** (ΔG only).

Similar results were obtained for the Pd/Se and Pt/S systems (ESI), illustrating lower energies of triplets than the separated doublet precursors, and very low activation energies for transformation to adducts comprised of M^{IV} and M^{II} fragments, with the overall process summarised in eq 4.

$$2\ [M^{III}Me_2(bipy)(EPh)]^\bullet \rightarrow M^{IV}Me_2(bipy)(EPh)_2 + M^{II}Me_2(bipy) \quad (4)$$

13a-c **17a-c** **1a-c**

As noted above, photochemical splitting of the dimers gives two doublets $[M^{III}Me_2(bipy)(EPh)]^\bullet$ (**13a-c**) where the doublets are oriented with adjacent 'MMe$_2$(bipy)' planes. It appears most likely that tumbling of doublets within the radical pair solvent cage allows facile formation of adducts **18a-c**, followed by $[EPh]^\bullet$ transfer with spin pairing to give adducts **19a-c**.

Conclusions

The overall 2e$^-$ oxidation of dimethyl(2,2'-bipyridine)platinum(II) (**1a**) and its palladium analogue (**1b**) with diphenyldiselenide to give octahedral metal(IV) complexes $MMe_2(bipy)(SePh)_2$ (**17a,b**) (eq 5) proceeds in a complex manner via oxidation state +III intermediates.

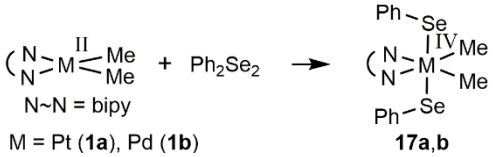

(5)

Oxidation to form M^{III} dimers $[MMe_2(bipy)(SePh)]_2$ (**11a,b**) occurs in 2e$^-$ oxidative transfer of $[PhSe]^+$ to a binuclear precursor adduct $[Pt^{II}Me_2(bipy)]_2$ (**4a,b**) (Scheme 4a). The M^{III}-M^{III} bonded dimers **11a,b** undergo photochemical excitation in the visible region to an excited state with M-M antibonding character (LUMO+2 for Pt, LUMO for Pd), allowing fragmentation to form doublet radicals $[M^{III}Me_2(bipy)(SePh)]^\bullet$ (**13a,b**) (Scheme 4b). Two doublets form a triplet adduct (**18a,b**) facilitating $[PhSe]^\bullet$ transfer between metal centres to give the metal(IV) product (**17a,b**) and metal(II) reactant (**1a,b**) (Scheme 4c), and **1a,b** is able to re-enter the sequence (Scheme 4a).

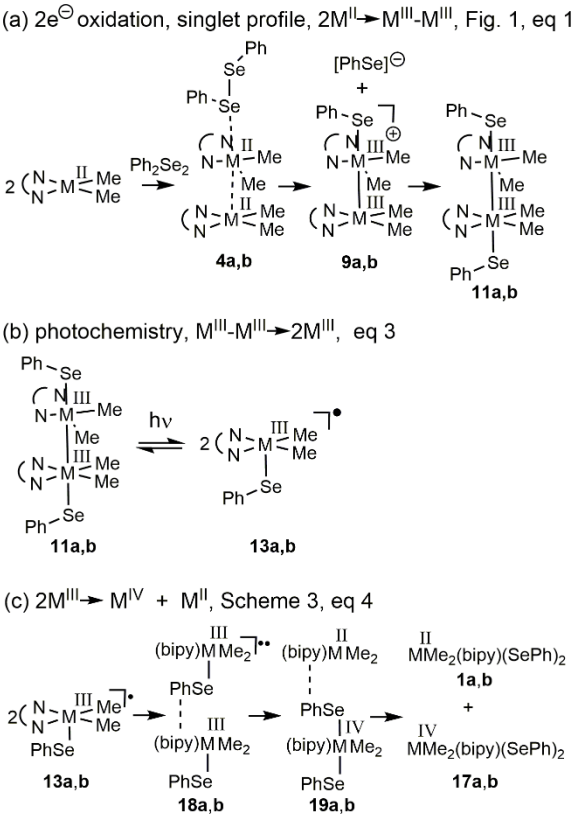

Scheme 4 Summary of the reaction sequence in formation of complexes $M^{IV}Me_2(bipy)(SePh)_2$ (**17a,b**), via M^{III} intermediates (**11a,b**), from $M^{II}Me_2(bipy)$ **(1a,b)** and Ph_2Se_2, with references to relevant Figures, Schemes and equations.

The complexity of the processes reported here, involving several classes of organometallic mechanism, of the apparently simple $2e^-$ oxidation of palladium(II) and platinum(II) complexes to the +IV oxidation state, illustrates the rich mechanistic options available in connecting oxidation states in organopalladium and platinum chemistry.

Conflicts of interest

There are no conflicts to declare.

Acknowledgements

We acknowledge support from the Australian Research Council and the Australian National Computing Infrastructure.

Notes and references

1 K.-T. Aye, J. J. Vittal and R. J. Puddephatt, *J. Chem. Soc., Dalton Trans*., 1993, 1835.
2 (a) A. J. Canty, H. Jin, B. W. Skelton and A. H. White, *Inorg. Chem*., 1998, **37**, 3975. (b) A. J. Canty and H. Jin, *J. Organomet. Chem*., 1998, **565**, 135. (c) A. J. Canty, M. C. Denney, J. Patel, H. Sun, B. W. Skelton and A. H. White, *J. Organomet. Chem*., 2004, **689**, 672.
3 A. Panunzi, G. Roviello and F. Ruffo, *Organometallics*, 2002, **21**, 3503.
4 Z. Zhuang, A. N. Herron, Z. Fan and J.-Q. Yu, *J. Am. Chem. Soc*., 2020, **142**, 6769.
5 K. J. Bonnington, M. C. Jennings and R. J. Puddephatt, *Organometallics*, 2008, **27**, 6521.
6 M. J. Frisch, G. W. Trucks, H. B. Schlegel, G. E. Scuseria, M. A. Robb, J. R. Cheeseman, G. Scalmani, V. Barone, G. A. Petersson, H. Nakatsuji, X. Li, M. Caricato, A. V. Marenich, J. Bloino, B. G. Janesko, R. Gomperts, B. Mennucci, H. P. Hratchian, J. V. Ortiz, A. F. Izmaylov, J.L. Sonnenberg, D. Williams-Young, F. Ding, F. Lipparini, F. Egidi, J. Goings, B. Peng, A. Petrone, T. Henderson, D. Ranasinghe, V. G. Zakrzewski, J. Gao, N. Rega, G. Zheng, W. Liang, M. Hada, M. Ehara, K. Toyota, R. Fukuda, J. Hasegawa, M. Ishida, T. Nakajima, Y. Honda, O. Kitao, H. Nakai, T. Vreven, K. Throssell, J. A. Montgomery, Jr., J. E.

Peralta, F. Ogliaro, M. J. Bearpark, J. J. Heyd, E. N. Brothers, K. N. Kudin, V. N. Staroverov, T. A. Keith, R. Kobayashi, J. Normand, K. Raghavachari, A. P. Rendell, J. C. Burant, S. S. Iyengar, J. Tomasi, M. Cossi, J. M. Millam, M. Klene, C. Adamo, R. Cammi, J. W. Ochterski, R. L. Martin, K. Morokuma, O. Farkas, J. B. Foresman, and D. J. Fox, *Gaussian 16, Revision B.01*; Gaussian, Inc., Wallingford CT, 2016.

7 *(a)* Y. Zhao, N. E. Schultz and D. G. Truhlar, *J. Chem. Theory Comput*., 2006, 2, 364. *(b)* Y. Zhao and D. G. Truhlar, *J. Chem. Phys*., 2006, 125, 194101. *(c)* Y. Zhao and D. G. Truhlar, *J. Phys. Chem. A*, 2006, 110, 13126.

8 H. Andrae, U. Haussermann, M. Dolg, H. Stolland and H. Preuss, *Theor. Chim. Acta,* 1990, **77**, 123.

9 (a) S. Ehrlich, J. Moellmann and S. Grimme, *Acc. Chem. Res*., 2013, **46**, 916. (b) J. Antony, R. Sure and S. Grimme, *Chem. Commun*., 2015, **51**, 1764.

10 F. Weigend, F. Furche and R. Ahlrichs, *J. Chem. Phys*., 2003, **119**, 12753.

11 J. W. Ochterski, J. W. *Thermochemistry in Gaussian*, Inc., Wallingford, CT, 2000.

12 (a)T. Yanai, D. P. Tew and N. C. Handy, *Chem. Phys. Lett*., 2004, **393**, 51. (b) C. J. Cramer and D. G. Truhlar, *Phys. Chem. Chem. Phys*., 2009, **11**, 10757.

13 S. Achar, V. J. Catalano, *Polyhedron*, 1997, **16**, 1550.

14 (a) J. F. Hartwig, K. S. Cook, M. Hapke, C. D. Incarvito, Y. Fan, C. E. Webster and M. B. Hall, *J. Am. Chem. Soc*., 2005, **127**, 2538. (b) C. S. Wei, C. A. Jiménez-Hoyos, M. F. Videa, J. F. Hartwig and M. B. Hall, *J. Am. Chem. Soc*., 2010, **132**, 3078.

15 A. Bondi, *J. Phys. Chem*., 1964, **68**, 441.

16 Technical Support, Gaussian Inc., Wallingford CT, 2016.

Text and graphic for contents page

Oxidative $[PhSe]^+$ transfer facilitates reaction of Ph_2Se_2 with $[M^{II}Me_2(bipy)]_2$ to give $[M^{III}Me_2(bipy)(SePh)]_2$, for which excitation by light to the M-M antibonding orbital releases $2[M^{III}Me_2(bipy)(SePh)]^{\bullet}$; the doublets react to give $M^{IV}Me_2(bipy)(SePh)_2$ and $M^{II}Me_2(bipy)$.